Conductivity and applications of Li-biphenyl-1,2-dimethoxyethane solution for lithium ion batteries*

Geng Chu(褚赓)[1], Bo-Nan Liu(刘柏男)[1], Fei Luo(罗飞)[2], Wen-Jun Li(李文俊)[1], Hao Lu(陆浩)[1], Li-Quan Chen(陈立泉)[1], and Hong Li(李泓)[1,†]

[1] *Beijing National Laboratory for Condensed Matter Physics, Institute of Physics, Chinese Academy of Sciences, Beijing* 100190, *China*
[2] *Department of Chemistry, Tsinghua University, Beijing* 100084, *China*

(Received 3 February 2017; revised manuscript received 21 March 2017; published online 6 June 2017)

The total conductivity of Li-biphenyl-1,2-dimethoxyethane solution ($Li_xBp(DME)_{9.65}$, Bp = biphenyl, DME = 1,2-dimethoxyethane, $x = 0.25$, 0.50, 1.00, 1.50, 2.00) is measured by impedance spectroscopy at a temperature range from 0 °C to 40 °C. The $Li_{1.50}Bp(DME)_{9.65}$ has the highest total conductivity 10.7 mS/cm. The conductivity obeys Arrhenius law with the activation energy ($E_{a(x=0.50)} = 0.014$ eV, $E_{a(x=1.00)} = 0.046$ eV). The ionic conductivity and electronic conductivity of $Li_xBp(DME)_{9.65}$ solutions are investigated at 20 °C using the isothermal transient ionic current (ITIC) technique with an ion-blocking stainless steal electrode. The ionic conductivity and electronic conductivity of $Li_{1.00}Bp(DME)_{9.65}$ are measured as 4.5 mS/cm and 6.6 mS/cm, respectively. The $Li_{1.00}Bp(DME)_{9.65}$ solution is tested as an anode material of half liquid lithium ion battery due to the coexistence of electronic conductivity and ionic conductivity. The lithium iron phosphate (LFP) and $Li_{1.5}Al_{0.5}Ti_{1.5}(PO_4)_3$ (LATP) are chosen to be the counter electrode and electrolyte, respectively. The assembled cell is cycled in the voltage range of 2.2 V–3.75 V at a current density of 50 mA/g. The potential of $Li_{1.00}Bp(DME)_{9.65}$ solution is about 0.3 V vs. Li^+/Li, which indicates the solution has a strong reducibility. The $Li_{1.00}Bp(DME)_{9.65}$ solution is also used to prelithiate the anode material with low first efficiency, such as hard carbon, soft carbon and silicon.

Keywords: lithium solution, ionic and electronic conductivity, flow lithium ion battery, prelithiation

PACS: 82.47.Aa, 82.45.Fk, 72.60.+g **DOI:** 10.1088/1674-1056/26/7/078201

1. Introduction

In 1936, researchers found that the alkali metal (Li, Na, K, etc.) could be dissolved in the ether solution containing aromatic compounds.[1] Weissman *et al.* proposed and certified that the dissolution was caught by electron transfer.[2–4] Hereafter the physical and chemical properties of this complex solution are studied continuously by researchers.[5,6] In recent years, the theoretical calculations of the interaction and structure between alkali metal, aromatic compounds and various ether molecules in the complex solution have been investigated.[7] In addition, the conductivity of the complex solution was measured.[8,9] However, no detailed analysis of the conductivity has been reported so far.

As there has been rapidly increasing demand of electric cars and hybrid vehicles in recent years, the study of electrochemical energy storage devices has attracted more and more attention. As a new battery technology, lithium ion flow battery combining the advantages of lithium ion battery and flow battery, is a kind of new green rechargeable battery with high energy density and low cost, in which the power and energy storage units are independent of each other.[10–12] The typical structure of a redox-flow battery contains two chambers: a positive chamber and a negative chamber, which are separated by an ion-exchange membrane.[13] The two chambers containing active species are circulated by the external circulating sub-system. The major problem of non-aqueous redox flow batteries is the poor rate capability, due to the low electronic and ionic conductivity and poor coulombic efficiency (CE) which results from the unstable solid electrolyte interface layer on the anode surface at low lithium intercalation voltage.[14,15]

Graphite is the most popular material as the anode electrode for lithium-ion batteries nowadays. A solid electrolyte interphase (SEI) film will form on the surface of the graphite anode at the first cycle. The formation of the SEI film consumes a certain amount of lithium provided from the cathode, which will decrease the actual energy density of the full battery.[16] Currently, the coulombic efficiency of the graphite anode at the first cycle is around 85%–95%. The main irreversible capacity loss is caused by the SEI formation. This is even worse for the next generation anode materials, such as hard carbon,[17] soft carbon,[18] silicon,[19,20] tin based compounds[21–23] etc. These anode materials show the low initial coulombic efficiency around 60%–80%. Therefore, it is necessary to develop an effective solution to compensate for the lithium consumed by the SEI formation. Many methods have been proposed to solve this problem, such as electrochemistry prelithiation,[24,25] adding a Li-rich cathode (i.e.,

*Project supported by the National Natural Science Foundation of China (Grant No. 52315206), the Ministry of Science and Technology of China (Grant No. 2016YFB0100100), and the Beijing Municipal Science and Technology Commission, China (Grant No. D151100003115003).

†Corresponding author. E-mail: hli@iphy.ac.cn

© 2017 Chinese Physical Society and IOP Publishing Ltd

Li_2NiO_2) in the cathode,[26] adding stabilized lithium metal powder (SLMP) in the anode,[27] and so on. However, most of these methods are not satisfactory for practical application due to the issues of production expansion and safety.

In this work, a series of experiments are designed to study the conductivity and applications of $Li_xBp(DME)_{9.65}$ solutions. Firstly, the total conductivities of the $Li_xBp(DME)_{9.65}$ ($x = 0.25, 0.50, 1.00, 1.50, 2.00$) solutions at various temperatures are measured by impedance spectroscopy. The electronic conductivities and ionic conductivities of $Li_xBp(DME)_{9.65}$ solutions are separated by ITIC measurement. Secondly, a half liquid battery with $Li_{1.00}Bp(DME)_{9.65}$ solution as the flow anode material is assembled and cycled. The LFP and LATP are chosen to be the cathode and electrolyte, respectively. Thirdly, the $Li_{1.00}Bp(DME)_{9.65}$ solution is also investigated as a prelithiation agent for hard carbon, soft carbon and nano-silicon.

2. Experiment

2.1. $Li_xBp(DME)_{9.65}$ solutions preparation

The $Li_xBp(DME)_{9.65}$ solutions were prepared in a glove box filled with argon. Different amounts of lithium metal (China Energy Lithium Co. Ltd, China), biphenyl (alfa Aesar, China) and DME (alfa Aesar, China) were prepared according to "x" of the $Li_xBp(DME)_{9.65}$ ($x = 0.25, 0.50, 1.00, 1.50, 2.00$) solutions. Then, biphenyl was dissolved in DME by magnetic stirring for 2 h at room temperature in a glass bottle. In order to increase the dissolution rate, the lithium metal could be cut into small pieces. Finally, the lithium metal pieces were put into the biphenyl DME solution with string for 2 h at room temperature.

2.2. Conductivity measurement

The $Li_xBp(DME)_{9.65}$ ($x = 0.25, 0.50, 1.00, 1.50, 2.00$) solutions were sealed in a glass bottle for the conductivity measurement. The cell had two stainless steel electrodes with an area of 0.5 cm^2 and a distance of 0.8 cm. An electrochemical workstation (Zahner IM6e) was used for impedance spectroscopy measurements. The data was recorded in the frequency range from 100 Hz to 8.0 MHz by applying an alternating voltage of 5 mV at different temperature (0–40 °C). The conductivity cell was calibrated by a standard 0.1 M potassium chloride solution at 25 °C. For the ITIC measurements, the voltage was 0.1 V between two electrodes and the current was recorded for 30 minutes at 20 °C.

2.3. Electrodes preparation

The LFP (BTR New Energy Material Co. Ltd, China) electrode was prepared by a slurry coating procedure. The slurry was composed of LFP as the active material, carbon black (alfa) as the conductivity additive and polyvinylidene fluoride (alfa) as the binder in a weight ratio of 80:10:10 dissolved in N-methyl pyrrolidone (alfa). Then the slurry was spread uniformly onto an aluminum foil and dried in a vacuum oven at 120 °C for 6 h. For the anodes, carboxymethylcellulose (CMC)/styrene-butadiene rubber (SBR) was chosen as the binder. The current collector was copper foil. The weight ratio of CMC and SBR was 2:3. The active materials of the anode were hard carbon (BTR New Energy Material Co. Ltd, China), soft carbon (BTR New Energy Material Co. Ltd, China), graphite (BTR New Energy Material Co. Ltd, China), and nano-silicon (alfa), respectively.

2.4. Prelithiation and electrochemical measurements of anodes

For the prelithiation process, the anode electrodes were immersed in the $Li_{1.00}Bp(DME)_{9.65}$ solution for 15 s, 40 s, 1 min, and 5 min, respectively. The electrodes were then washed by dimethyl carbonate to remove the excess biphenyl. The electrochemical measurements of the electrodes were carried out with 2032 coin cells using lithium metal as the counter electrode. The solution of 1.0 M $LiPF_6$ and vinylene carbonate (2% in volume) in ethylene carbonate and dimethyl carbonate (1:1 in volume) was served as the electrolyte. The cells were galvanostatically charged and discharged at a current density of 100 mA/g between 0.005 V and 2.0 V (vs. Li^+/Li) on the Land BA2100A battery testing system (Wuhan, China) at room temperature.

2.5. Assembling and electrochemical measurements of the half liquid battery

For the half liquid battery, a new structure of battery is shown in Fig. 1. The $Li_{1.00}Bp(DME)_{9.65}$ solution was used as the anode and the copper foam as the current collector. We selected the LFP electrode to be the counter cathode, and use the LATP solid state electrolyte pellet to separate the cathode and anode.[28] The solution of 1.0 M $LiPF_6$ in ethylene carbonate and dimethyl carbonate (1:1 in volume) was served as the electrolyte for the cathode side. The battery was galvanostatically charged and discharged at a current density of 50 mA/g between 2.20 V and 3.75 V (vs. Li^+/Li) at room temperature by a Land BA2100A battery testing system (Wuhan, China).

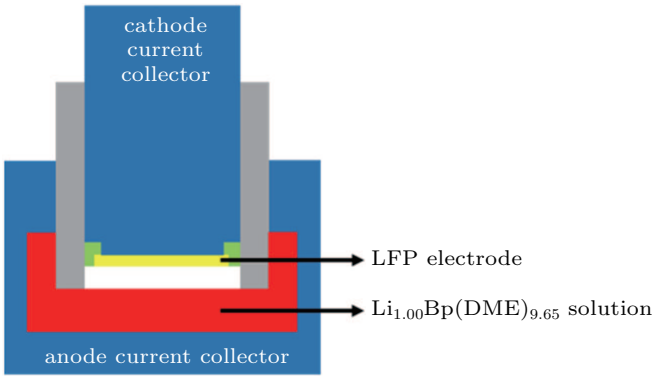


Fig. 1. (color online) Structure of the flow battery. The Blue part is stainless steel, Grey parts are Teflon, the Red one is $Li_{1.00}Bp(DME)_{9.65}$ solution, the White part is LATP, Yellow is the LFP electrode and Green is the electrolyte.

3. Results and discussion

3.1. Isothermal transient ionic current (ITIC)

The current versus time curve at 0.1 V (20 °C) between two stainless steel electrodes of five kinds of $Li_xBp(DME)_{9.65}$ (x = 0.25, 0.50, 1.00, 1.50, 2.00) solutions are shown in Fig. 2(a). When $x \geq 1.00$, the current decreases quickly and stabilizes around a current value. For others, the current does not change with time obviously. The almost invariant current indicates low ionic conductivity for x below 1.00, which is due to the electronic conductor and ionic insulator property of stainless steel electrodes. The rapid decline of the current indicates the existence of ionic transport. The electronic conductivity always exists from the final value of the current of these curves.

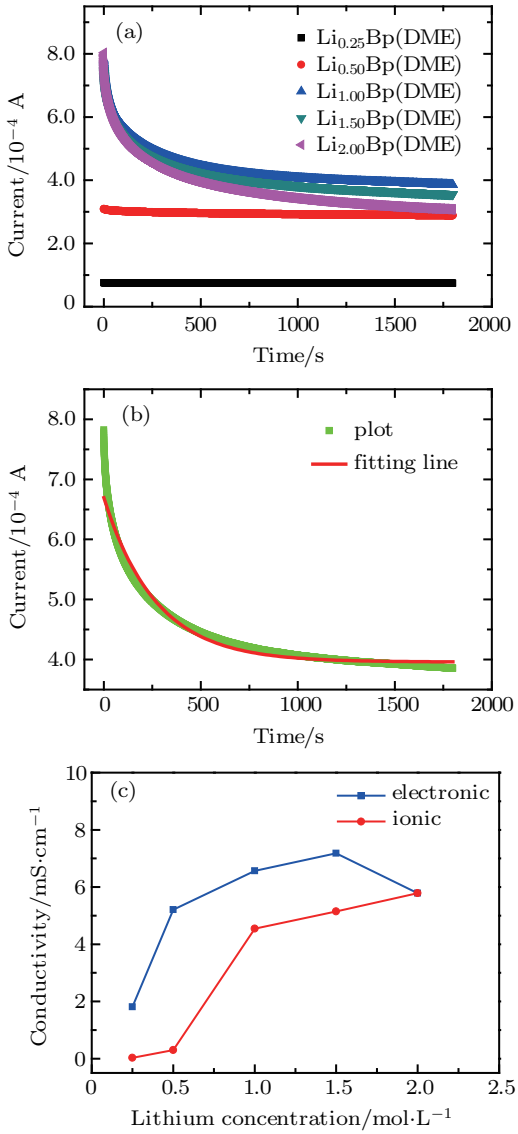


Fig. 2. (color online) (a) The current versus time of $Li_xBp(DME)_{9.65}$ (x = 0.25, 0.50, 1.00, 1.50, 2.00) solutions at 20 °C during the 0.1 V step. (b) The current versus time of $Li_{1.00}Bp(DME)_{9.65}$ solution at 20 °C during the 0.1 V step, experimental data (blue) and fitting line (red). (c) The fitting result of electronic conductivities and ionic conductivities of $Li_xBp(DME)_{9.65}$ (x = 0.25, 0.50, 1.00, 1.50, 2.00) solutions at 20 °C.

The ionic conductivities and electronic conductivities of the $Li_xBp(DME)_{9.65}$ solutions are achieved by fitting the curves shown in Fig. 2(b)[29,30] with the following formula:

$$J(t)=\frac{\sigma_{dc,e^-}U}{L}+\frac{\sigma_{dc,Li^+}U}{L}\exp\left(-\frac{\mu_{Li^+}U}{L^2}t\right), \quad (1)$$

where J is the current density, L is the distance between the two stainless steel electrodes and μ_{Li^+} is the lithium ion mobility, σ_{dc,e^-} and σ_{dc,Li^+} denote the electronic conductivity and ionic conductivity, respectively, t is the time and U is the voltage between two electrodes.

The fitting result is shown in Fig. 2(c). The electronic conductivity enhances as the lithium concentration increases up to 7.2 mS/cm. However, the rising speed slows down gradually. The ionic conductivity enhances with the increasing of lithium concentration in this work. It is noticed that the ionic conductivity is several orders of magnitude lower than the electronic conductivity for the $Li_{0.50}Bp(DME)_{9.65}$ and $Li_{0.25}Bp(DME)_{9.65}$. It reveals that the electrons migrate more easily in the solution than in ions. This is an amazing result since nearly all reported solutions have negligible electronic conductivity at room temperature. With the lithium concentration increasing, the ionic conductivity is close to the electronic conductivity. Compared with the electronic conductivity, the ionic conductivity always shows a lower value when the lithium concentration is lower than $Li_{2.00}Bp(DME)_{9.65}$.

3.2. Impedance spectroscopy

The impedance spectrum of $Li_xBp(DME)_{9.65}$ (x = 0.25, 0.50, 1.00, 1.50, 2.00) solutions at 20 °C are shown in Fig. 3(a). The conductivities are calculated by the following formula:

$$\sigma_{total}=\frac{K}{R}, \quad (2)$$

where σ_{total} is the conductivity of the $Li_xBp(DME)_{9.65}$ solution tested by impedance spectroscopy, R is the impedance from the impedance spectroscopy, and K is the electrode coefficient of the stainless steel counter electrode calibrated by 0.1 M potassium chloride solution at 25 °C.

The σ_{total} versus lithium concentration is shown in Fig. 3(b). The σ_{total} enhances as the lithium concentration increases up to 10.7 mS/cm. The rising speed reduces obviously as "x" is higher than 1.00. With the increasing of lithium content increasing, the conductions of ions and electrons are influenced by the interaction between them. The relation between total conductivity and temperature is shown in Fig. 3(c). The σ_{total} of $Li_xBp(DME)_{9.65}$ solutions enhance in higher temperature. A perfect linear relationship is obtained. This means that the system obeys the Arrhenius law, which allows us to estimate the activation energy ($E_{a(x=0.50)}$ = 0.014 eV, $E_{a(x=1.00)}$ = 0.046 eV). The higher ionic conductivity implies more correlation between activation energy and temperature. Compared

with $LiPF_6$-PC (0.12 eV), the lower $E_{a(x=1.00)}$ is due to the low viscosity of DME.[31,32] The slope of fitting lines is much lower for the $Li_{0.50}Bp(DME)_{9.65}$ and $Li_{0.25}Bp(DME)_{9.65}$ compared with the higher lithium concentration ones. This is reasonable that the ionic conductivity in the high concentration system is more significant than that in the dilute solution system.

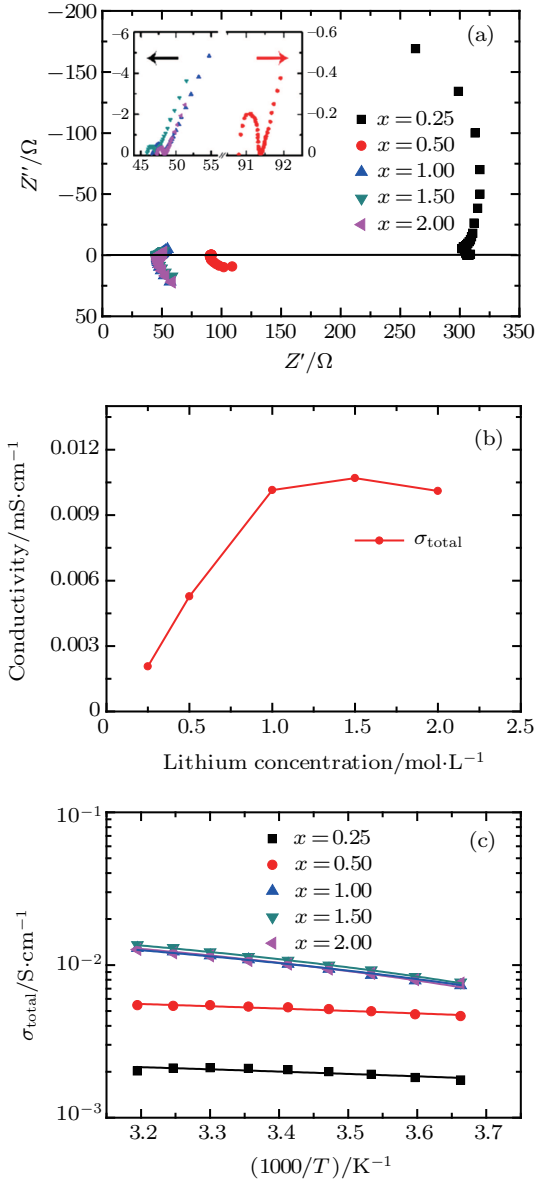


Fig. 3. (color online) (a) The impedance spectrum of $Li_xBp(DME)_{9.65}$ ($x = 0.25, 0.50, 1.00, 1.50, 2.00$) solutions at 20 °C. The inset shows the local amplification. (b) The total conductivities of $Li_xBp(DME)_{9.65}$ solutions from the impedance spectroscopy. (c) Temperature versus total conductivities of $Li_xBp(DME)_{9.65}$ solutions.

3.3. Half liquid battery

The charge–discharge curve of the half liquid battery at the first cycle is shown in Fig. 4(a). The specific capacity of LFP is 130 mAh/g, which is lower than 160 mAh/g in normal Li-ion batteries, due to the large cell polarization (0.3 V) and low charge cut-off voltage 3.75 V. The first coulombic efficiency is 95%, which is obviously higher than that of the graphite-based anode battery due to the presence of the SEI formation. The charge and discharge potential platforms of the full battery are 3.3 V and 3.0 V respectively, and the LFP versus Li^+/Li is 3.45 V.[33] Therefore, the potential of $Li_{1.00}Bp(DME)_{9.65}$ solution versus Li^+/Li is about 0.3 V. This illustrates that the full cell has high voltage and high energy density. The polarization between the charge curve and discharge curve is as large as 0.3 V. One reason for the large polarization is the low ionic conductivity of the LATP solid electrolyte pellet.

The cycling performance of the half liquid battery is shown in Fig. 4(b) which does not satisfy the specific capacity decay of 10 mAh/g after 20 cycles. This is due to the reactions between the LATP and the $Li_{1.00}Bp(DME)_{9.65}$ solution. The low redox potential of $Li_{1.00}Bp(DME)_{9.65}$ solution (0.3 V versus Li^+/Li) indicates strong reducibility. The LATP is not stable below 1.5 V versus Li^+/Li as is well known.[28]

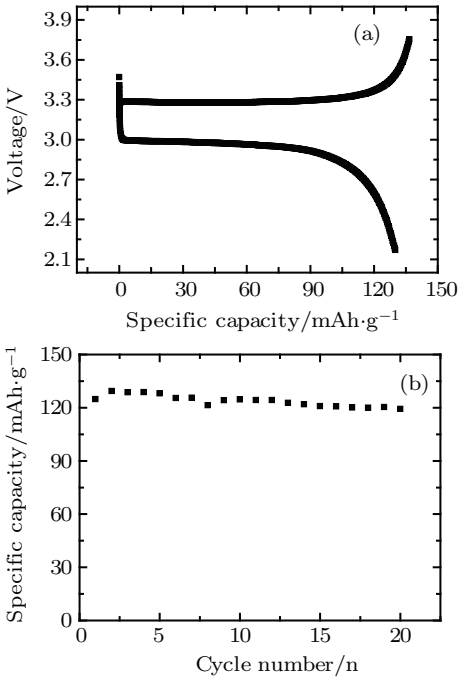


Fig. 4. The performance of the LFP-$Li_{1.00}Bp(DME)_{9.65}$ solution battery: (a) Charge–discharge curve of the first cycle; (b) cycling performance.

3.4. Chemical prelithiation

As a result of the strong reducibility of $Li_{1.00}Bp(DME)_{9.65}$ solution (0.3 V versus Li^+/Li), it is a convenient solution agent for prelithiation. Figure 5 shows the electrochemical performance of anode materials with and without lithiation of graphite, nano-silicon, soft carbon and hard carbon. For the graphite, the first coulombic efficiencies are 88.6% (without lithiation) and 89.3% (after lithiation for 40 s) as shown in Fig. 5(a). This result indicates that the presence of $Li_{1.00}Bp(DME)_{9.65}$ solution is difficult to lithiate the graphite anode due to the low lithiation voltage of graphite.[34] The potential is lower than the $Li_{1.00}Bp(DME)_{9.65}$ solution

voltage (0.3 V). For the soft carbon, the first coulombic efficiencies are 86.1% (without lithiation), 94.2% (after lithiation for 15 s), 107.5% (after lithiation for 40 s), 112.7% (after lithiation for 1 min) and 124.9% (after lithiation for 5 min), which is shown in Fig. 5(b). For the hard carbon, the values of the first coulombic efficiency are 74.8% (without lithiation), 91.2% (after lithiation for 15 s), 95.2% (after lithiation for 40 s), 95.8% (after lithiation for 1 min), and 161.7% (after lithiation for 5 min) as shown in Fig. 5(c). For the hard carbon and soft carbon, these results show that their first coulombic efficiencies can be improved obviously. Figure 5(d) tells us that the first coulombic efficiency of nano-silicon has improved less (3.9%) than soft carbon (21.4%) and hard carbon (20.4%) after a 40 s lithiation process. This difference indicates that the kinetic of lithiation into nano-silicon is not as good as hard carbon and soft carbon. Figures 5(e)–5(g) demonstrate that the cycling performance of the nano-silicon, hard carbon and soft carbon do not deteriorate after the lithiation process.

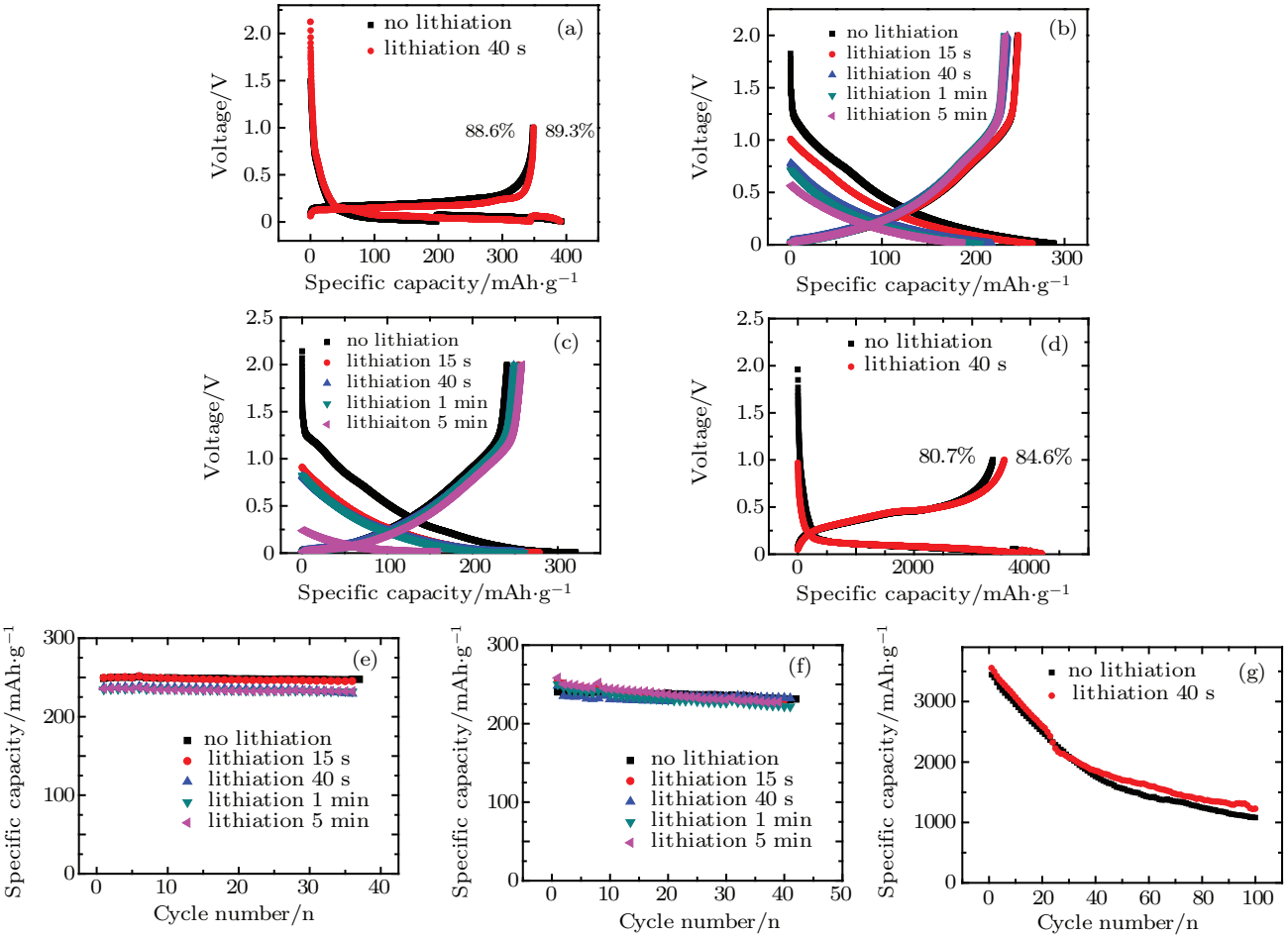


Fig. 5. (color online) Half battery performance of lithiated graphite (a), soft carbon ((b), (e)), hard carbon ((c), (f)), nano-silicon ((d), (g)) electrodes. (a), (b), (c), (d) are the first charge-discharge curves. (e), (f), (g) are the cycling performance.

4. Conclusion and perspectives

The conductivities of $Li_xBp(DME)_{9.65}$ ($x = 0.25$, 0.50, 1.00, 1.50, 2.00) solutions are measured by impedance spectroscopy and ITIC. The $Li_{1.50}Bp(DME)_{9.65}$ has the highest total conductivity of 10.7 mS/cm. The conductivity displays an Arrhenius law temperature dependence with the activation energies $E_{a(x=0.50)} = 0.014$ eV and $E_{a(x=1.00)} = 0.046$ eV. The temperature dependent conduction mechanism is different from the metal and semiconductor, similar to the electrolyte solution. The ionic conductivity and electronic conductivity of $Li_{1.00}Bp(DME)_{9.65}$ are 4.5 mS/cm and 6.6 mS/cm respectively. The electronic conductivity dominates as x is less than 1.00. The values of both ionic and electronic conductivity of such a solution at room temperature are quite high. Although it is known that there is charge transfer between dissolved lithium and molecular, the mechanism of the total ionic and electronic transport at the molecular level is not very clear and it is valuable to investigate such an interesting and unusual system.

Our results demonstrate that the $Li_{1.00}Bp(DME)_{9.65}$ solution can be used as an anode and prelithiation agent. Both are very important for developing new battery and new processing techniques.

References

[1] Scott N D, Walker J F and Hansley V L 1936 *J. Am. Chem. Soc.* **58** 2442
[2] Walker J F and Scott N D 1938 *J. Am. Chem. Soc.* **60** 951
[3] Bergmann E and Bergmann F 1937 *J. Am. Chem. Soc.* **59** 1443
[4] Jeanes A and Adams R 1937 *J. Am. Chem. Soc.* **59** 2608
[5] Chu T L and Yu S C 1954 *J. Am. Chem. Soc.* **76** 3367
[6] Holmeswalker W A and Ubbelohde A R 1954 *J. Chem. Soc.* **720**
[7] Liu N, Li H, Jiang J, Huang X J and Chen L Q 2006 *J. Phys. Chem. B* **110** 10341
[8] Tan K S, Grimsdale A C and Yazami R 2012 *J. Phys. Chem. B* **116** 9056
[9] Tan K S and Yazami R 2015 *Electrochim. Acta* **180** 629
[10] Huang Q, Li H, Gratzel M and Wang Q 2013 *Phys. Chem. Chem. Phys.* **15** 1793
[11] Zhao Y, Ding Y, Li Y, Peng L, Byon H R, Goodenough J B and Yu G 2015 *Chem. Soc. Rev.* **44** 7968
[12] Duduta M, Ho B, Wood V C, Limthongkul P, Brunini V E, Carter W C and Chiang Y M 2011 *Adv. Energy Mater.* **1** 511
[13] Huang Q Z and Wang Q 2016 *Chin. Phys. B* **25** 7
[14] Chen Y C, Wu M X, Ren Y K, Kang L B, Li Y J, Han L, Lin D Y and Wang Q P 2012 *Adv. Technol. Electral. Eng. Energ.* **31** 3
[15] Feng C M, Chen Y C, Han L, Gong Y, Cserhati C and Csik A 2015 *Energ. Stor. Sci. Technol.* **4** 3
[16] Verma P, Maire P and Novák P 2010 *Electrochim. Acta* **55** 6332
[17] Wang Q, Li H, Chen L Q and Huang X J 2001 *Carbon* **39** 2211
[18] Bonino F, Brutti S, Piana M, Natale S, Scrosati B, Gherghel L and Mullen K 2006 *Electrochim. Acta* **51** 3407
[19] Li H, Huang X J, Chen L Q, Wu Z G and Liang Y 1999 *Electrochem. Solid State Lett.* **2** 547
[20] Liu X, Xie K, Zheng C M and Wang J 2011 *Acta Phys. Sin.* **60** 6 (in Chinese)
[21] Shi S L, Liu Y G, Zhang J Y and Wang T H 2009 *Chin. Phys. B* **18** 4564
[22] Li J, Ru Q, Hu S J and Guo L Y 2014 *Acta Phys. Sin.* **63** 9 (in Chinese)
[23] Li J, Ru Q, Sun D W, Zhang B B, Hu S J and Hou X H 2013 *Acta Phys. Sin.* **62** 8 (in Chinese)
[24] Zhang J, Shi Z and Wang C 2014 *Electrochim. Acta* **125** 22
[25] Zhang J, Wu H, Wang J, Shi J and Shi Z 2015 *Electrochim. Acta* **182** 156
[26] Park H, Yoon T, Kim Y U, Ryu J H and Oh S M 2013 *Electrochim. Acta* **108** 591
[27] Forney M W, Ganter M J, Staub J W, Ridgley R D and Landi B J 2013 *Nano Lett.* **13** 4158
[28] Zhou W, Wang S, Li Y, Xin S, Manthiram A and Goodenough J B 2016 *J. Am. Chem. Soc.* **138** 9385
[29] Watanabe M, Rikukawa M, Sanui K and Ogata N 1985 *J. Appl. Phys.* **58** 736
[30] Zhang S S and Wan G X 1993 *J. Appl. Polym. Sci.* **48** 405
[31] Xu K 2004 *Chem. Rev.* **104** 4303
[32] Nishida T, Nishikawa K and Fukunaka Y 2008 *ECS Trans.* **6** 1
[33] Yamada A, Chung S C and Hinokuma K 2001 *J. Electrochem. Soc.* **148** A224
[34] Dahn J R 1991 *Phys. Rev. B* **44** 9170